JOC Article
pubs.acs.org/joc

Fullerene/Thiol-Terminated Molecules

Yasuhiro Shirai,[†,‡] Jason M. Guerrero,[†] Takashi Sasaki,[†] Tao He,[†] Huanjun Ding,[§] Guillaume Vives,[†] Byung-Chan Yu,[†,∥] Long Cheng,[†] Austen K. Flatt,[†] Priscilla G. Taylor,[†] Yongli Gao,[§] and James M. Tour*[,†]

[†]*Department of Chemistry, Smalley Institute for Nanoscale Science and Technology, Rice University, MS-222, 6100 Main Street, Houston, Texas 77005,* [‡]*ICYS-MANA, National Institute for Materials Science, 1-1 Namiki, Tsukuba, Ibaraki, 305-0044, Japan,* [§]*Department of Physics and Astronomy, University of Rochester, Rochester, New York 14627, and* [∥]*Department of Chemistry, Mokwon University, Daejon, 302-729, Republic of Korea*

tour@rice.edu

Received August 13, 2009

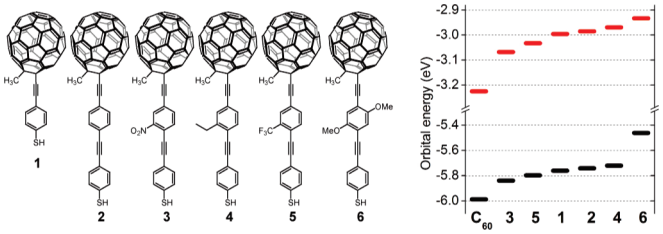

A series of fullerene-terminated oligo(phenylene ethynylene) (OPEs) have been synthesized for potential use in electronic or optoelectronic device monolayers. Electronic properties such as the energy levels and the distribution of HOMOs and LUMOs of fullerene-terminated OPEs have been calculated using the ab initio method at the B3LYP/6-31G(d) level. The calculations have revealed the concentration of frontier orbitals on the fullerene cage and a narrow distribution of HOMO−LUMO energy gaps. Ultraviolet photoelectron spectroscopy and inverse photoemission spectroscopy studies have been performed to further examine the electronic properties of the fullerene-terminated OPEs on gold surfaces. The obtained broad photoelectron spectra suggest that there are strong intermolecular interactions in the fullerene self-assembled monolayers, and the small bandgap (∼1.5 eV), determined by the photoelectron spectroscopy, indicates the unique nature of the fullerene-terminated OPEs in which the C_{60} moiety can be connected to the Au surface through the conjugated OPE backbone.

Introduction

Design, synthesis, and application of conjugated molecules have received great attention since the suggestion in 1974 of the miniaturization of electronic circuits to a molecular scale.[1] A variety of molecules have been synthesized,[2−4] and the characterization of these nanoscale electronic wires have shown promising results such as in solar harvesting devices[5] and other optoelectronic systems.[6] Our early approaches to molecular electronics using oligo(phenylene ethynylene) OPE devices[7−10] gained attention after the successful demonstration of switching effects using this class of compounds.[11−13] To further advance the development of OPE-based monlayers, we have

(1) Aviram, A.; Ratner, M. A. *Chem. Phys. Lett.* **1974**, *29*, 277–283.
(2) Mullen, K.; Wegner, G. *Electronic Materials: The Oligomer Approach*; Wiley-VCH: Weinheim, 1998.
(3) Gholami, M.; Tykwinski, R. R. *Chem. Rev.* **2006**, *106*, 4997–5027.
(4) Bunz, U. H. F. *Chem. Rev.* **2000**, *100*, 1605–1644.
(5) Lembo, A.; Tagliatesta, P.; Guldi, D. M.; Wielopolski, M.; Nuccetelli, M. *J. Phys. Chem. A* **2009**, *113*, 1779–1793.
(6) Slepkov, A. D.; Hegmann, F. A.; Eisler, S.; Elliott, E.; Tykwinski, R. R. *J. Chem. Phys.* **2004**, *120*, 6807–6810.
(7) Tour, J. M.; Rawlett, A. M.; Kozaki, M.; Yao, Y. X.; Jagessar, R. C.; Dirk, S. M.; Price, D. W.; Reed, M. A.; Zhou, C. W.; Chen, J.; Wang, W. Y.; Campbell, I. *Chem Eur. J.* **2001**, *7*, 5118–5134.
(8) James, D. K.; Tour, J. M. *Aldrichim. Acta* **2006**, *39*, 47–56.
(9) James, D. K.; Tour, J. M. *Mol. Wires: Design Prop.* **2005**, *257*, 33–62.
(10) Tour, J. M., *Molecular Electronics: Commercial Insights, Chemistry, Devices, Architecture and Programming*; World Scientific: River Edge, NJ, 2003.
(11) Chen, J.; Reed, M. A.; Rawlett, A. M.; Tour, J. M. *Science* **1999**, *286*, 1550–1552.
(12) Chen, J.; Wang, W.; Reed, M. A.; Rawlett, A. M.; Price, D. W.; Tour, J. M. *Appl. Phys. Lett.* **2000**, *77*, 1224–1226.
(13) Tour, J. M.; Cheng, L.; Nackashi, D. P.; Yao, Y. X.; Flatt, A. K.; St Angelo, S. K.; Mallouk, T. E.; Franzon, P. D. *J. Am. Chem. Soc.* **2003**, *125*, 13279–13283.

DOI: 10.1021/jo901701j Published on Web 09/16/2009

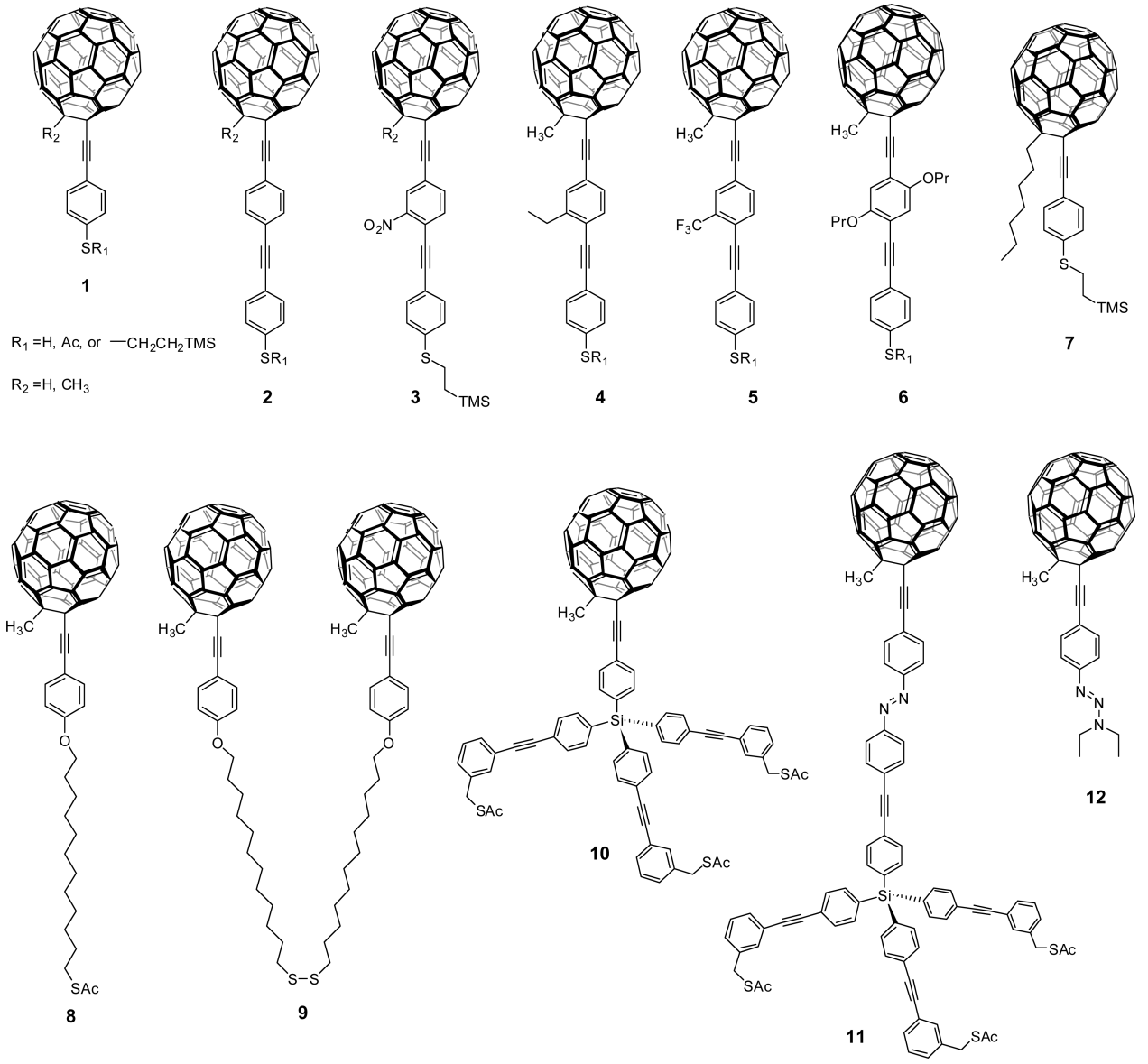

FIGURE 1. Fullerene-terminated molecules presented in this work.

investigated fullerene−OPE hybrid devices (Figure 1). Fullerenes have gained considerable attention since their discovery due to their unusual structure and optical and electrical properties, and there has been a tremendous amount of research aimed at developing new fullerene-based materials with novel and potentially useful applications.[14,15] Fullerenes are also attractive candidates for anchoring molecule wires on electrode surfaces because of their high affinity for noble metals and large contacting area. The efficacy of the fullerene-based anchoring group have been demonstrated in single-molecule electronic measurements.[16] The unique combination of the well-known thiol-based self-assembled monolayer (SAM) chemistry[14] with the advantageous properties of fullerene derivatives could lead to advances in this field.[15,16] To that end, we have demonstrated the self-assembly of fullerene−OPE hybrid devices on Au surfaces and delineated the specific mechanisms associated with self-assembly of fullerene−OPE hybrids.[17]

Here we expand the synthesis of a series of fullerene-terminated molecules by introducing a variety of functional groups and describe their electronic properties with the aid of theoretical calculations and ultraviolet photoelectron spectroscopy (UPS) and inverse photoemission spectroscopy (IPES) methods. The variety of the fullerene-terminated molecules with thiol and protected thiol alligator clips can be easily expanded using our in situ ethynylation method.[18] Moreover, the fine-tuning of the electronic properties in the fullerene-terminated OPEs was successfully demonstrated with a combination of molecular design and theoretical calculations. A clear correlation was

(14) Love, J. C.; Estroff, L. A.; Kriebel, J. K.; Nuzzo, R. G.; Whitesides, G. M. *Chem. Rev.* **2005**, *105*, 1103–1169.
(15) Mirkin, C. A.; Caldwell, W. B. *Tetrahedron* **1996**, *52*, 5113–5130.
(16) (a) Zeng, C. G.; Wang, H. Q.; Wang, B.; Yang, J. L.; Hou, J. G. *Appl. Phys. Lett.* **2000**, *77*, 3595–3597. (b) Martin, C. A; Ding, D.; Sørensen, J. K.; Bjørnholm, T.; van Ruitenbeek, J. M.; van der Zant, H. S. J. *J. Am. Chem. Soc.* **2008**, *130*, 13198–13199.
(17) Shirai, Y.; Cheng, L.; Chen, B.; Tour, J. M. *J. Am. Chem. Soc.* **2006**, *128*, 13479–13489.
(18) Shirai, Y.; Zhao, Y. M.; Cheng, L.; Tour, J. M. *Org. Lett.* **2004**, *6*, 2129–2132.

observed between the electron-donating or -accepting characteristics of the functional groups and the HOMO/LUMO energy levels. The attachment of C_{60} with alkynes is also interesting in that one can expect periconjugation[19,20] effects due to the close proximity between the fullerene cage and the OPE π systems. The UPS and IPES studies are evidence that the C_{60} moiety can be connected to the Au surface through the conjugated OPE backbone. The estimated HOMO−LUMO bandgap (~1.5 eV) by UPS and IPES was measurable and clearly smaller than the bandgap of C_{60}−SAMs in which the C_{60} moieties were attached to Au surfaces with a saturated carbon backbone.[21]

Results and Discussion

Synthesis of Fullerene-Terminated OPEs 1 and 7. The fullerene−OPE hybrids **1** and **7** can be synthesized in a single step from the known compound **13**[22] using the in situ ethynylation method[18] with moderate yields (Scheme 1). The ethyl-TMS group (−CH_2CH_2TMS) was employed as the protecting group for the sulfur atom because it can tolerate the in situ ethynylation reaction using lithium hexamethyldisylazide (LHMDS). Once the fullerene moiety is attached, the ethyl-TMS protecting group can be easily removed using tetrabutylammonium fluoride (TBAF) in THF (**1-Me-SH**) or converted to the acetyl group (**1-Me-SAc**) using $AgBF_4$ and acetyl chloride (AcCl).[23] The in situ deprotection and self-assembly of the ethyl-TMS protected derivatives have been shown previously;[24] however, in our hands, it was difficult to obtain consistent assembly results.[25] We also found in our previous work that the thiol esters (−SAc) were more convenient and reliable.[17] The functional group attached on the fullerene cage can be modified in the ethynylation step by quenching the fullerene anions with the appropriate alkyl iodide or a proton. In the synthesis of **7**, 1-iodoheptane was used to introduce a bulky group at the fullerene site to reduce the cross-sectional mismatch that was one of the causes for the head-to-tail assemblies in fullerene SAMs.[17] Unfortunately, this synthesis approach proved to be difficult, with a low yield presumably because of the lower reactivity of the 1-iodoheptane toward the fullerene anions.

Synthesis of Fullerene-Terminated OPEs 2−6. A series of fullerene-terminated compounds **2**−**6** were synthesized via Pd-catalyzed coupling reactions and removal of the TMS groups followed by the fullerene coupling reaction (Scheme 2). With this synthesis scheme, simple modification of the functional groups in the compound **14** can result in the rapid generation of the wide variety of the fullerene-terminated molecules. We have previously demonstrated the combinatorial synthesis of OPE tetramers on a solid support.[26] In this work, we were able

SCHEME 1. Synthesis of the Fullerene-Terminated Compounds 1 and 7

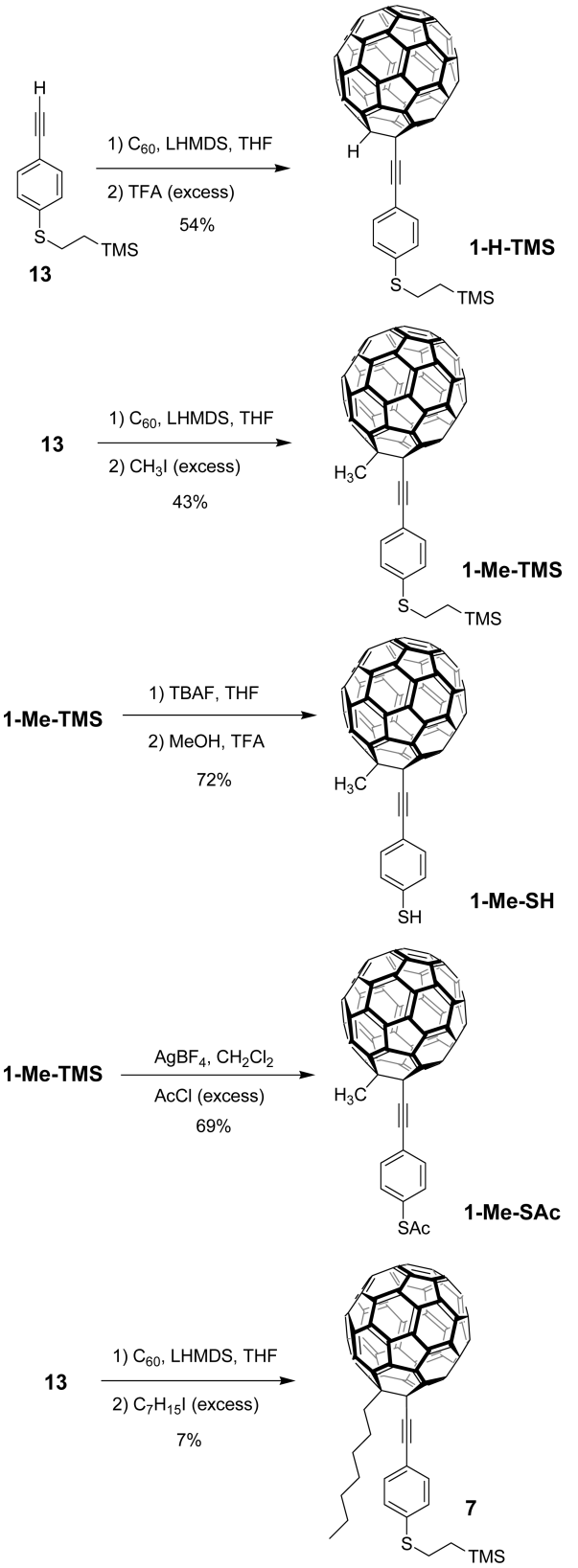

to synthesize −H (neutral), −Et (electron rich), $-CF_3$ (electron deficient), −OPr (electron rich), and $-NO_2$ (electron deficient) derivatives of the fullerene-terminated systems **2**−**6**. The ethyl-TMS protecting groups for the sulfur atom were

(19) Hamasaki, R.; Ito, M.; Lamrani, M.; Mitsuishi, M.; Miyashita, T.; Yamamoto, Y. *J. Mater. Chem.* **2003**, *13*, 21–26.
(20) Zhao, Y. M.; Shirai, Y.; Slepkov, A. D.; Cheng, L.; Alemany, L. B.; Sasaki, T.; Hegmann, F. A.; Tour, J. M. *Chem.—Eur. J.* **2005**, *11*, 3643–3658.
(21) Patnaik, A.; Setoyama, H.; Ueno, N. *J. Chem. Phys.* **2004**, *120*, 6214–6221.
(22) Yu, C. J.; Chong, Y. C.; Kayyem, J. F.; Gozin, M. *J. Org. Chem.* **1999**, *64*, 2070–2079.
(23) Grundberg, H.; Andergran, M.; Nilsson, U. J. *Tetrahedron Lett.* **1999**, *40*, 1811–1814.
(24) Creager, S.; Yu, C. J.; Bamdad, C.; O'Connor, S.; MacLean, T.; Lam, E.; Chong, Y.; Olsen, G. T.; Luo, J. Y.; Gozin, M.; Kayyem, J. F. *J. Am. Chem. Soc.* **1999**, *121*, 1059–1064.
(25) Dirk, S. M.; Price, D. W.; Chanteau, S.; Kosynkin, D. V.; Tour, J. M. *Tetrahedron* **2001**, *57*, 5109–5121.
(26) Hwang, J. J.; Tour, J. M. *Tetrahedron* **2002**, *58*, 10387–10405.

SCHEME 2. Synthesis of the Fullerene-Terminated Molecules 2−6

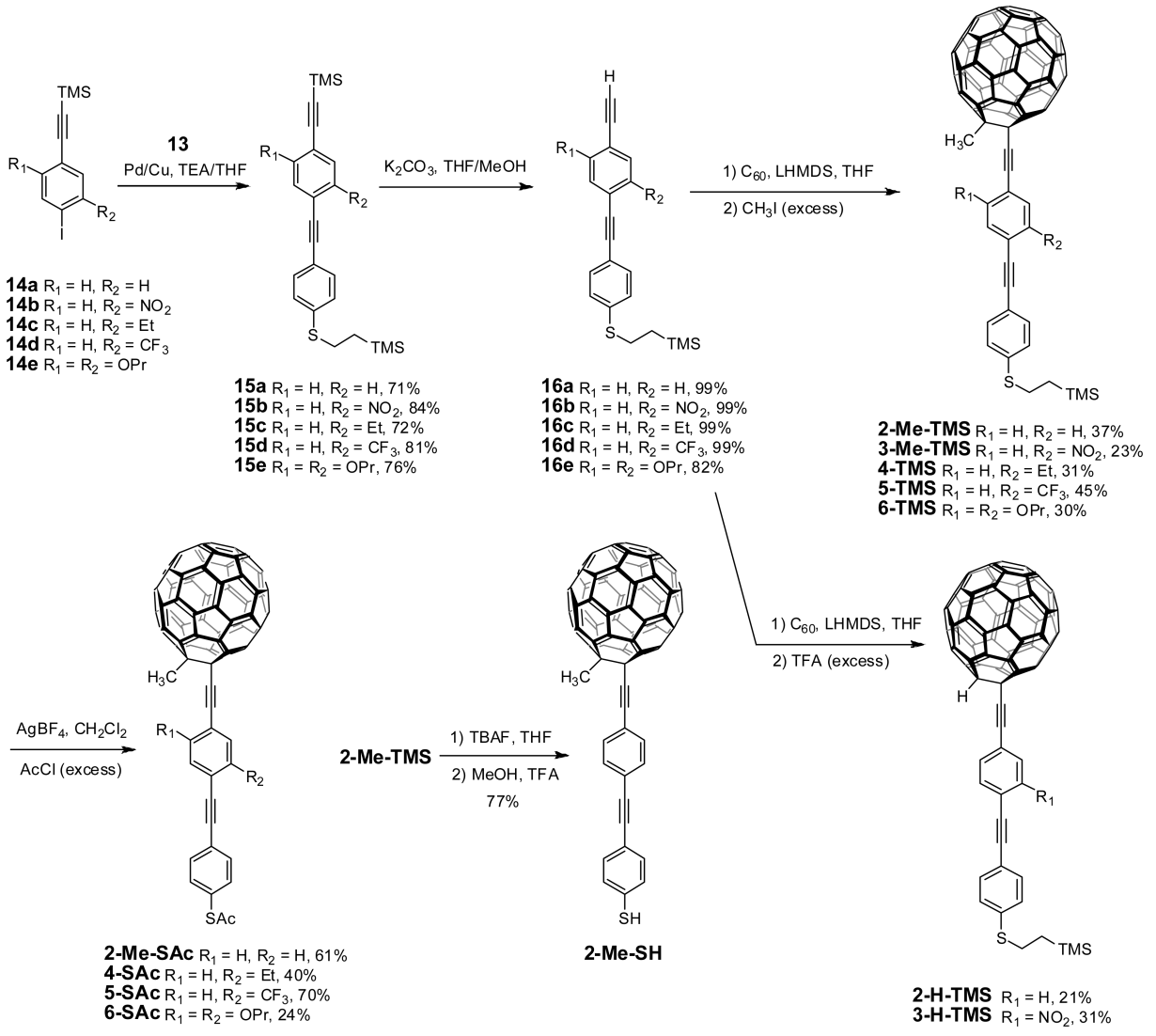

removed as before, except for the nitro derivative **3**, that was found to undergo side reactions to form insoluble materials during the deprotection step.

Synthesis of Fullerene-Terminated Alkyl Thiol 8 and Disulfide 9. Fullerene-terminated compounds incorporating a long alkyl chain were prepared as thiol ester **8** and disulfide **9** (Scheme 3). The 4-iodophenol was alkylated with 1,12-dibromododecane, and the monofunctionalized bromododecane **17** was isolated using chromatography. The ethyl-TMS protected sulfur atom was introduced by the lithiation of 2-(trimethylsilyl)-ethanethiol followed by a condensation reaction with bromododecane **17**, giving the product **18**. After the introduction of the terminal alkyne via Pd-catalyzed reaction with trimethylsilylacetylene (TMSA) and the removal of the TMS group, the fullerene moiety was coupled to give the fullerene-terminated alkyl thiol **21**. The sulfur atom protecting group was converted from ethyl-TMS to the thiol ester with the same strategy as in previous reactions to give the product **8**. Basic deprotection of the thiol ester **8** and oxidative coupling of the resulting thiol in air can easily generate the disulfide **9**.

Synthesis of Fullerene-Tripods 10 and 11. Fullerene-terminated compounds incorporating a tripod base were also synthesized (Schemes 4−6). The ethyl-TMS-protected sulfur atom was introduced by the lithiation of 2-(trimethylsilyl)-ethanethiol followed by a condensation reaction with 3-iodobenzyl bromide (**22**) affording the product **23**. Each leg of the tripod base (**25**) was obtained by a Pd-catalyzed reaction with TMSA followed by the removal of the TMS group, and then the legs (**25**) were coupled to the center part (**26**) to give the ethoxyl-terminated tripod **27**. The aryllithium generated from the bromide **28** displaces the ethoxyl group of **27** to give the product **29**. Finally, the tripod **30** was obtained after deprotection of the terminal alkyne. The fullerene tripod **10** was obtained after the in situ ethynylation of fullerenes and the conversion of the sulfur protecting groups using the same strategies with $AgBF_4$. The fullerene tripod with azobenzene functionality (**11**) was also synthesized from the tripod **30** by introducing the azobenzene moiety **31**[27] before the fullerene coupling and the protecting group exchange reaction (Scheme 6).

Synthesis of the Fullerene−Triazene Hybrid 12. The fullerene−triazene hybrid **12** can be easily synthesized from the

(27) Yu, B. C.; Shirai, Y.; Tour, J. M. *Tetrahedron* **2006**, *62*, 10303–10310.

SCHEME 3. Synthesis of the Fullerene-Terminated Alkyl Thiol 8 and Disulfide 9

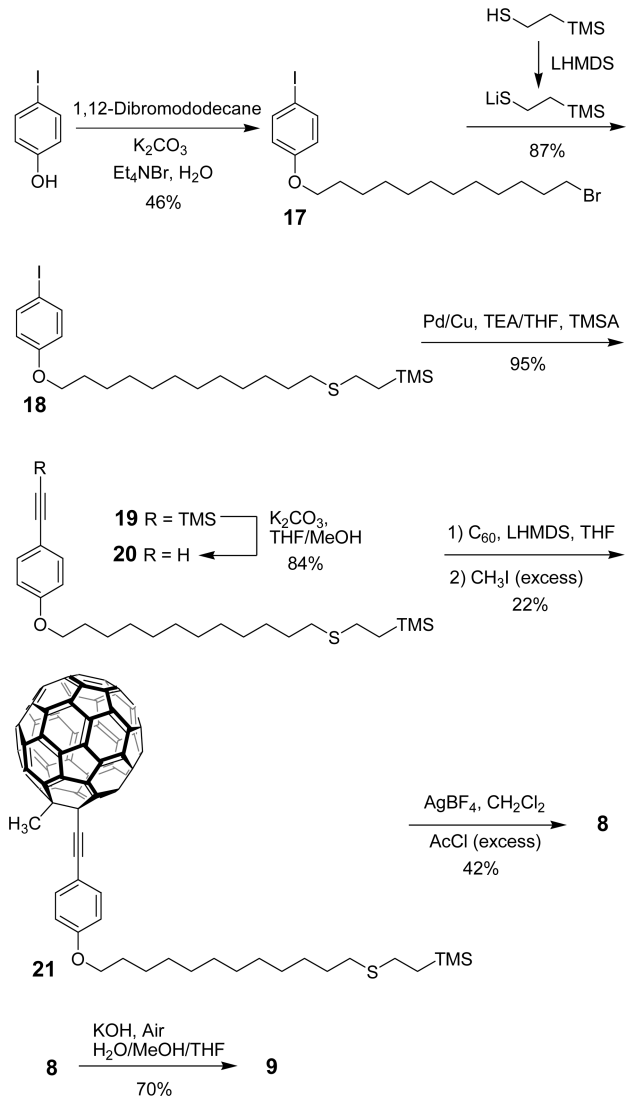

triazene **35** with a terminal alkyne using the in situ ethynylation method (Scheme 6). This strategy can be useful to assemble fullerene-terminated molecules on silicon surfaces.[28]

Theoretical Study on Fullerene-Terminated OPEs. The molecular orbital (MO) level is an important concept in explaining the fundamental behaviors of molecules, such as reactivity and kinetics. Furthermore, MO theory has been utilized as a powerful tool in the field of molecular electronics to describe charge-transfer processes on molecules. Electron transfer through molecules can be influenced by several factors such as molecular length, conformation, and various functional groups present within the molecule, and these factors eventually determine the frontier MOs such as the highest occupied MO (HOMO), lowest unoccupied MO (LUMO), and HOMO−LUMO gap energies.[29] Thus, it is quite common to extract trends in molecular behavior based on the MOs. For example, a smaller HOMO−LUMO gap can generally provide higher charge transport efficiency.[30] Molecules with deep-lying HOMO and LUMO levels can possibly result in better candidates for n-type organic semiconductors. The spatial distribution or extent of these MOs within the molecule is also important because the rectifying behaviors of molecules can be predicted.[31,32] Unfortunately, although MO theory is of immense utility, popular computational methods such as the B3LYP/6-31G(d) protocol cannot provide accurate (absolute) MO energy values. Nevertheless, the method is quite reliable for predicting molecular geometry and total energies.[33] We calculated total energies using B3LYP/6-31G(d) implemented in the Gaussian03 program, and geometry optimizations were done using the HF/3-21G* level of theory. The calculated frontier MO energies (HOMO and LUMO eigenvalues in the total energy calculation) for our fullerene-terminated OPEs **1**−**6** are tabulated along with the similar OPEs without C_{60} for comparison (Figure 2 and Table 1). In order to minimize calculation time, the propoxyl groups of **6** were replaced by methoxyl substituents for the calculation. The frontier MOs for the pristine C_{60} was also calculated to compare with our devices. It is clear from Table 1 that the HOMO−LUMO gaps (HLG)s of our fullerene-terminated compounds **1**−**5** (2.75−2.77 eV) are almost identical to that of pristine C_{60} (2.76 eV) even though our devices contain various functional groups with different electron-donating (−Et for **4**) and -accepting (−NO_2 and −CF_3 for **3** and **5**, respectively) characters or length of OPEs (one benzene ring for **1** and two rings for **2**). This is unusual compared with common OPE-based devices (**2**$_{Ph}$, **3**$_{Ph}$, **6**$_{Ph}$, see Figure 2 for structures), whose HLGs vary depending on the functional groups attached to the OPE backbone. Only the molecule with −OMe groups (**6**) gave a unique HLG (2.53 eV), which was the smallest of all. On the other hand, reasonable correlations between these electron-donating or -accepting characters of functional groups and HOMO/LUMO energy levels are clearly observed (Figure 2). Both HOMO and LUMO levels are aligned in the order of increasing electron-donating characters, −NO_2 < −CF_3 < −H < −Et < −OMe groups. The molecule with the nitro group (**3**) has the lowest HOMO and LUMO levels, and the molecule with methoxyl groups (**6**) gives the highest energy levels for both HOMO and LUMO. The size of the OPE backbone has almost no effect because compounds **1** and **2** share almost identical HOMO and LUMO levels. The HOMO and LUMO levels of pristine C_{60} are deeper than that of our devices by ∼0.2 eV, and this calculation result suggests that the electron-accepting power of fullerene is reduced when it is functionalized. This is a physically observable phenomenon, which we and other groups have previously reported in the study of fullerene-OPE hybrid devices using cyclic voltammetry.[16] The redox waves for fullerene derivatives always shift toward more negative potentials relative to pristine C_{60}, possibly due to the decrease of π-delocalization on the fullerene cage after the introduction of two sp^3 carbon atoms.

(28) Chen, B.; Flatt, A. K.; Jian, H. H.; Hudson, J. L.; Tour, J. M. *Chem. Mater.* **2005**, *17*, 4832–4836.
(29) Zhang, G.; Musgrave, C. B. *J. Phys. Chem. A* **2007**, *111*, 1554–1561.
(30) Ishii, H.; Sugiyama, K.; Ito, E.; Seki, K. *Adv. Mater.* **1999**, *11*, 605–+.
(31) Mizuseki, H.; Niimura, K.; Majumder, C.; Kawazoe, Y. *Comput. Mater. Sci.* **2003**, *27*, 161–165.
(32) Majumder, C.; Mizuseki, H.; Kawazoe, Y. *J. Phys. Chem. A* **2001**, *105*, 9454–9459.
(33) Zhan, C. G.; Nichols, J. A.; Dixon, D. A. *J. Phys. Chem. A* **2003**, *107*, 4184–4195.

SCHEME 4. Synthesis of the Fullerene Tripod 10

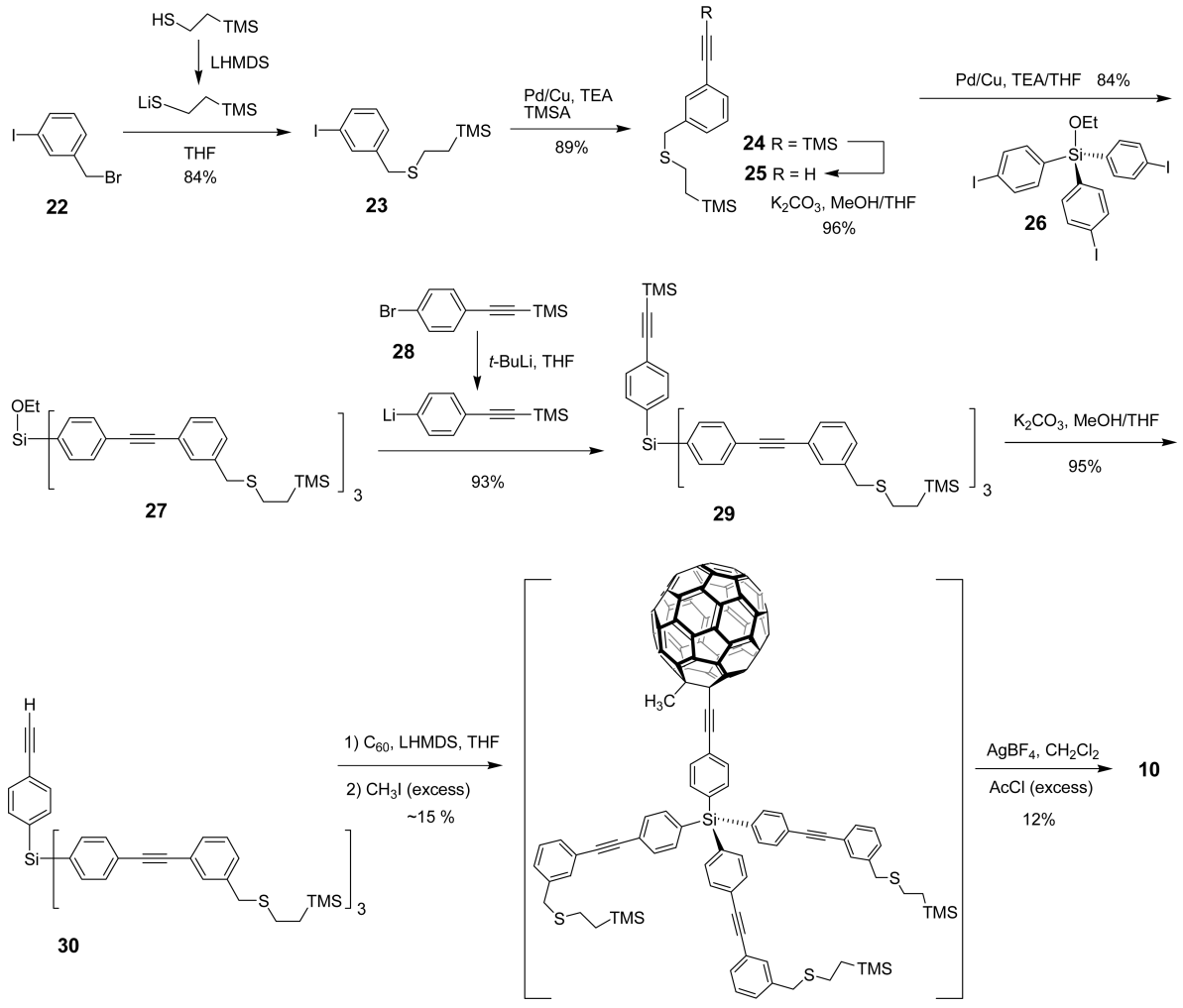

The examination of the spatial distribution of these MOs suggests that the frontier MOs in these fullerene-terminated molecules are dominated by the fullerene-related MOs. This can be demonstrated when these frontier MOs are plotted on molecules (Figure 3). Except for compound **6**, all frontier MOs reside predominantly on the fullerene cage, giving a narrow distribution of HLGs for fullerene-terminated OPEs.

Ultraviolet Photoelectron Spectroscopy and Inverse Photoemission Spectroscopy Rsults on Fullerene-Terminated OPE. The electronic structure of the fullerene-terminated OPE monolayer on the Au surface was examined. Figure 4 shows the distribution of the occupied and empty electronic states determined by the UPS and IPES, respectively. The simulated density of states (DOS) of the model compound (inset of Figure 4) was also plotted along with the experimental spectra. The simulated DOS was shifted for the best fit with the experimental spectra, and the vertical bars along with the DOS spectrum show the positions of the calculated MOs. The convolution of the MOs was performed using a Gaussian function with fwhm of 0.5 eV. The MO calculation was performed by applying B3LYP/LanL2DZ theory to the compound **2-Me-S** adsorbed at the 3-fold hollow site of the Au cluster (inset of Figure 4). The small Au cluster containing three gold atoms was used as the Au surface for the calculation because we are interested in the qualitative picture of MOs on surfaces. The strength of the small cluster approach has been justified with theoretical studies of self-assembled monolayers on metal surfaces.[21,34−36] During the structure optimization using the HF/LanL2DZ method, the Au−Au bond distances were fixed at 2.884 Å and equivalent S−Au distances were maintained. All other parameters were allowed to relax during the structure optimization. The optimized molecular structure is shown in the inset of Figure 4.

The work function of the clean Au substrate was 5.2 eV in our work, and it was decreased to 4.4 eV after the SAM formation. The decrease of the work function by ~0.8 eV is in accord with previous studies of self-assembled monolayers on metal surfaces.[21,30] The ionization potential (IP), electron affinity (EA), and bandgap (Eg) energies were estimated to be 5.2, 3.7, and 1.5 eV, respectively, from the onset of the photoelectron spectra. The observed UPS spectrum was broad comparing to that of the simulated DOS spectrum. The broadening can be a result of the strong intermolecular interactions in the SAM. Our previous study on fullerene

(34) Johansson, A.; Stafstrom, S. *Chem. Phys. Lett.* **2000**, *322*, 301–306.
(35) Seminario, J. M.; Zacarias, A. G.; Tour, J. M. *J. Am. Chem. Soc.* **1999**, *121*, 411–416.
(36) Vondrak, T.; Wang, H.; Winget, P.; Cramer, C. J.; Zhu, X. Y. *J. Am. Chem. Soc.* **2000**, *122*, 4700–4707.

SCHEME 5. Synthesis of the Fullerene Tripod 11

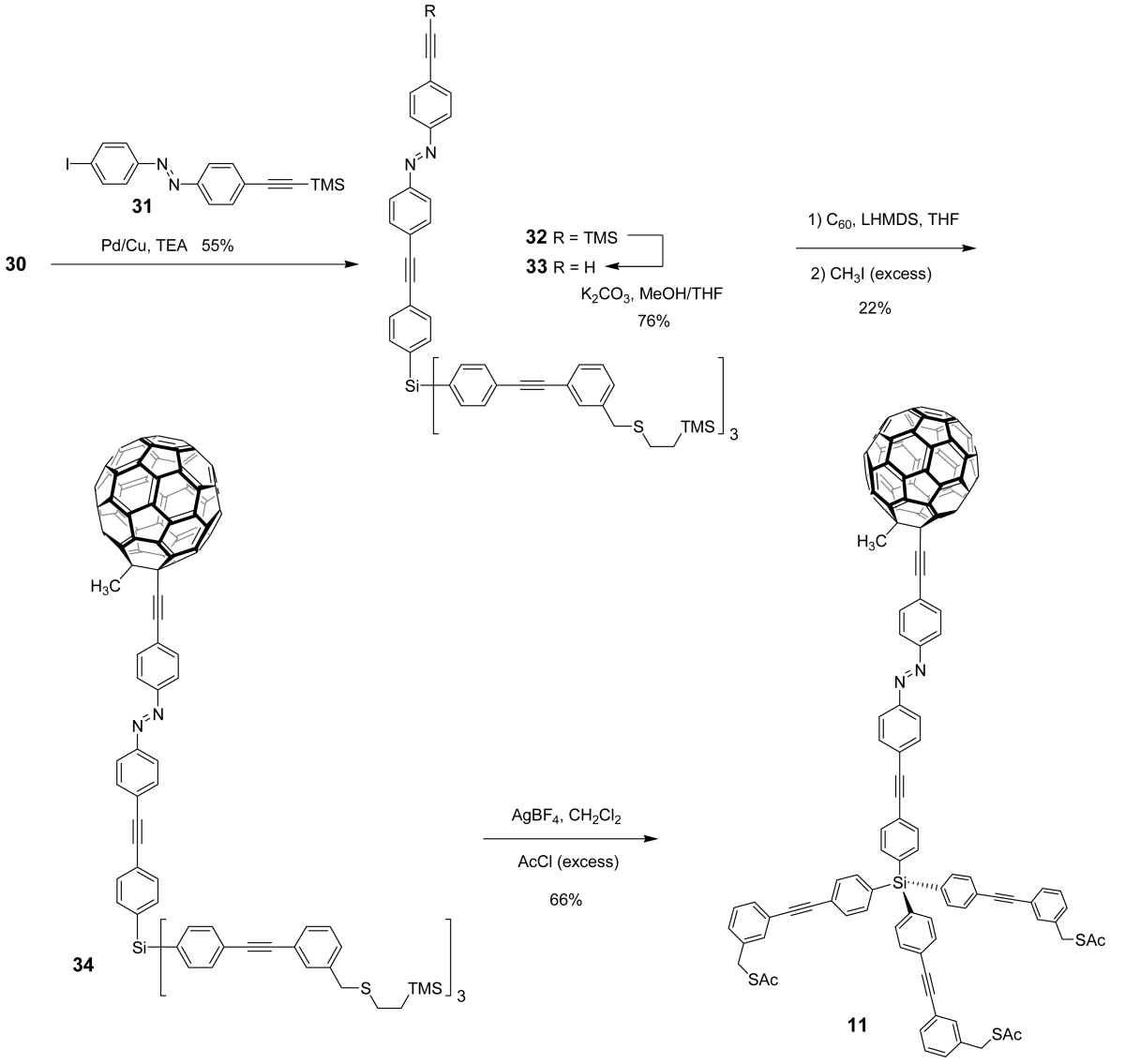

SCHEME 6. Synthesis of the Fullerene-Terminated Device 12

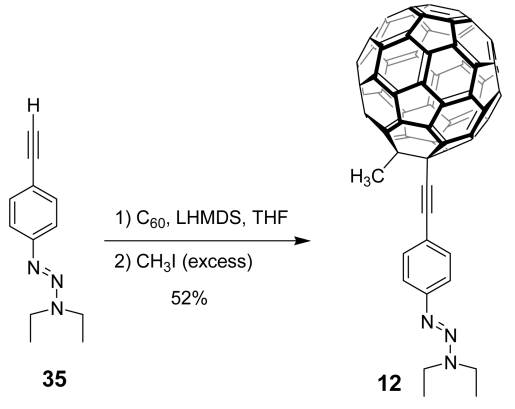

SAMs revealed the existence of mixed species such as head-to-tail assemblies due to the strong fullerene−Au and/or fullerene−fullerene interactions. For **2-Me-SAc**, about 30% of the sulfur atoms in the SAM were found to be in an unbound state using XPS analysis.[17] The majority of molecules (70%) were found to be in the bound state, attached on the gold surface by S−Au bonding. The structure of this bound species is expected to be similar to the model shown in the inset of Figure 4.[34,21] Thus, the observed photoelectron spectra should be the sum of the signals from the 70% bound and 30% unbound species in slightly different electronic and/or chemical environments, resulting in the rather broad spectrum. Although this situation makes detailed analysis of the UPS and IPES spectra difficult, the observed bandgap (1.5 eV) is measurable. The bandgap energy of 3.2 eV was estimated using UPS and IPES for C_{60} monolayers on Au surfaces[37] and 2.7 eV for the C_{60}-SAMs on Au using XPS and UPS.[21] In the later example, the C_{60} moiety was connected to the Au surface through a saturated carbon backbone. The observed smaller bandgap for our system is presumably due to the unique nature of fullerene-terminated OPEs, in which the C_{60} moiety can be connected to the Au surface through the conjugated OPE

(37) Ohno, T. R.; Chen, Y.; Harvey, S. E.; Kroll, G. H.; Weaver, J. H.; Haufler, R. E.; Smalley, R. E. *Phys. Rev. B* **1991**, *44*, 13747–13755.

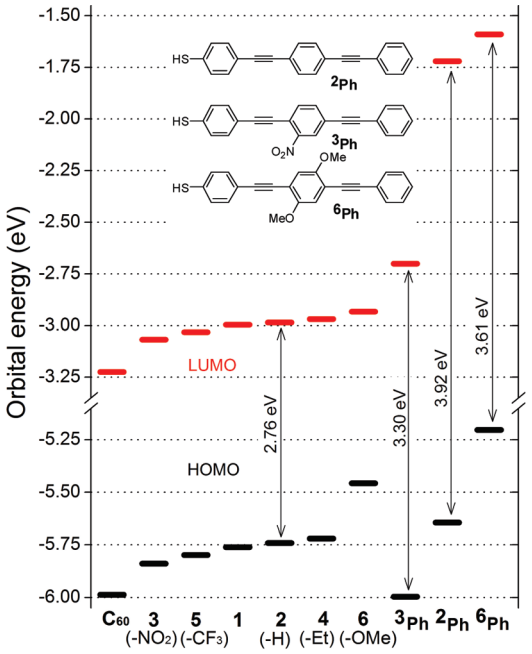

FIGURE 2. Calculated MO energy levels. The inset shows chemical structures for $\mathbf{2}_{Ph}$, $\mathbf{3}_{Ph}$, and $\mathbf{6}_{Ph}$. The structures of **1**−**6** are shown in Figure 1.

TABLE 1. Molecular Orbital Energies Calculated Using B3LYP/6-31G(d) Theory[a]

	energies (eV)		
compd	HOMO	LUMO	HOMO−LUMO gap
C_{60}	−5.99	−3.23	2.76
1	−5.76	−3.00	2.76
2 (−H)	−5.74	−2.99	2.76
3 ($-NO_2$)	−5.84	−3.07	2.77
4 (−Et)	−5.72	−2.97	2.75
5 ($-CF_3$)	−5.80	−3.03	2.76
6 (−OMe)	−5.46	−2.93	2.53
$\mathbf{2}_{Ph}$	−5.64	−1.72	3.92
$\mathbf{3}_{Ph}$	−6.00	−2.70	3.30
$\mathbf{6}_{Ph}$	−5.20	−1.59	3.61

[a]For the structures of **1**−**6**, see Figure 1. The structures of $\mathbf{2}_{Ph}$, $\mathbf{3}_{Ph}$, and $\mathbf{6}_{Ph}$ are shown in Figure 2.

backbone. The previous study on the reduction of the bandgap for C_{60} on metal surfaces has been explained in terms of Fermi-level alignment resulting from the mixing between the LUMO and filled metal states.[37] A similar mechanism can be applicable to our system with the fullerene-terminated OPEs on Au surfaces.

Conclusions

In this paper, we have reported efficient synthesis routes for the generation of a variety of fullerene-terminated compounds (Figure 1). Theoretical studies using DFT calculations have been performed to reveal the electronic nature of those fullerene-terminated OPEs. The calculation indicated that the frontier MOs of fullerene-terminated OPEs reside mainly on the fullerene cage and give the narrow distribution of HLG values regardless of the functional groups of the OPE moiety. The fine-tuning of the electronic properties in the fullerene-terminated OPEs was successfully demonstrated with the combination of molecular design and theoretical calculations.

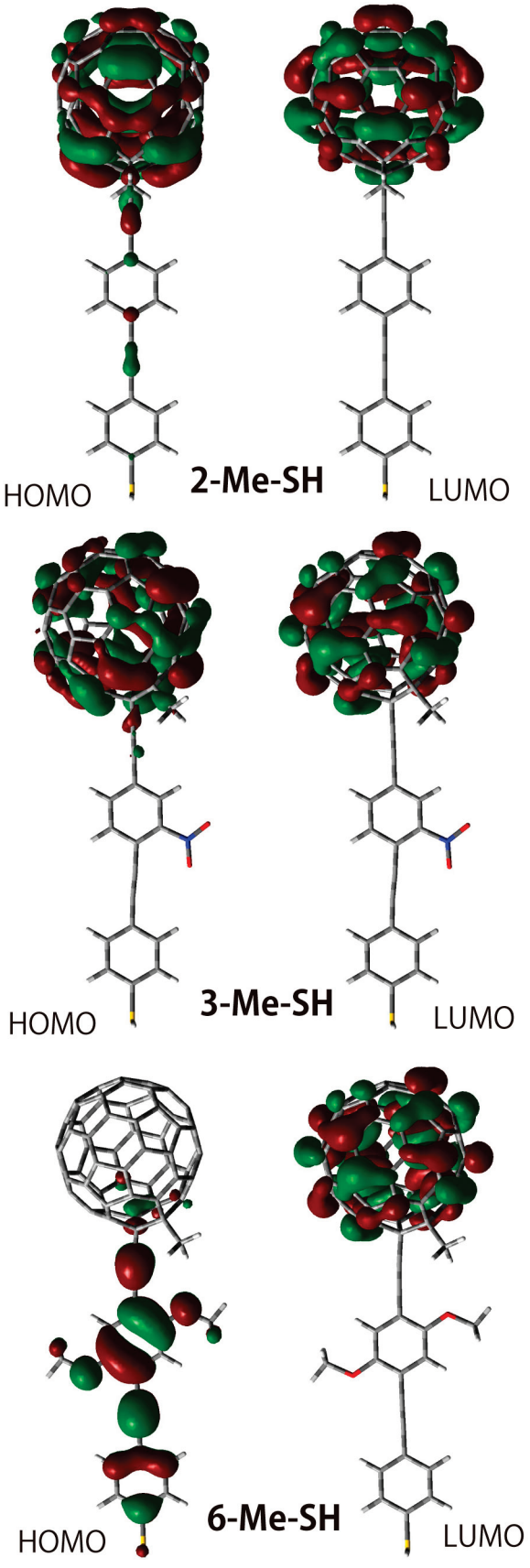

FIGURE 3. HOMO and LUMO molecular orbitals of representative fullerene-terminated OPEs.

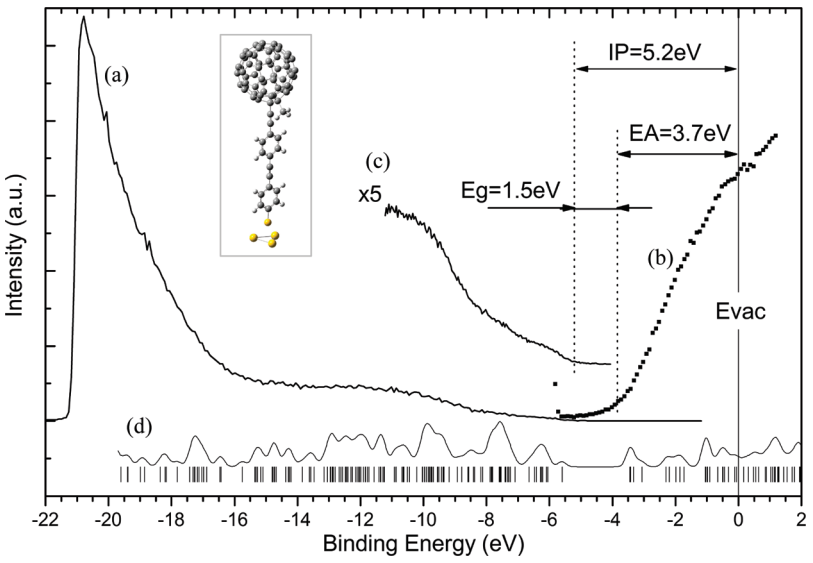

FIGURE 4. (a) UPS and (b) IPES spectra of **2-Me-SAc** assembled on the Au surface. The inset shows the molecular conformation of **2-Me-S** on Au cluster that was used for the simulation of DOS. (c) UPS spectrum enlarged 5 times in vertical scale. (d) Simulated DOS of the model system (inset) with the vertical bars representing MO energies obtained by DFT method.

A clear correlation was observed between the electron-donating or -accepting characteristics of the functional groups and the HOMO/LUMO energy levels. The electronic structure of fullerene-terminated OPEs on Au surfaces was also studied using UPS and IPES methods. The broad nature of the UPS and IPES spectra can be an indication of strong intermolecular interactions, a result which agrees with our previous findings on the self-assembly of these fullerene-terminated molecules on Au surfaces.[17] The observed small bandgap (1.5 eV) shows the unique nature of our fullerene-terminated OPEs, in which the C_{60} moiety can be coupled to the Au surface through the conjugated OPE backbone.

Experimental Section

Materials. The synthesis of compounds **1-Me-xxx**, **2-Me-xxx**, **8**−**10**, and **13** have been detailed in the literature.[17] Precursors **14a**−**e**,[26] **15a**,[38] **15e**,[38] **16a**,[38] **16e**,[38] **31**,[27] and **35**[39] were prepared according to literature procedures. All reactions were performed under an atmosphere of nitrogen unless stated otherwise. Reagent-grade diethyl ether and tetrahydrofuran (THF) were distilled from sodium benzophenone ketyl. Triethylamine (TEA) and CH_2Cl_2 were distilled over CaH_2. Fullerene (99.5+% pure) was purchased from MTR Ltd. and used as received. LHMDS (1 M solution in THF) and TBAF (1 M solution in THF) were obtained from Aldrich and used as received. Flash column chromatography was performed using 230−400 mesh silica gel from EM Science. Thin-layer chromatography was performed using glass plates precoated with silica gel 40 F_{254} purchased from EM Science. Melting points were uncorrected. Ultrasonicated fullerene slurry in THF was prepared in general ultrasonic cleaners.

Ultraviolet Photoelectron Spectroscopy (UPS) and Inverse Photoemission Spectroscopy (IPES). Photoemission spectroscopy of occupied and unoccupied states of the system was performed using a VG ESCA Lab system equipped with both UPS and IPES.[40−42] The spectrometer chamber of the UHV system had a base pressure of 8×10^{-11} Torr. Occupied states spectra were obtained by UPS using the unfiltered He I line (21.2 eV) of a discharge lamp with the samples biased at −5.0 V to avoid the influence of the detector work function and to observe the true low energy secondary cutoff. The typical instrumental resolution for UPS measurements ranges from ~0.03 to 0.1 eV with photon energy dispersion of less than 20 meV. Unoccupied states were measured by IPES using a custom-made spectrometer composed of a commercial Kimball Physics ELG-2 electron gun and a bandpass photon detector. IPES was done in the isochromat mode using a photon detector centered at a fixed energy of 9.8 eV. The combined resolution (electron + photon) of the IPES spectrometer was determined to be ~0.6 eV from the width of the Fermi edge measured on a clean polycrystalline Au film. The UPS and IPES energy scales were aligned by measuring the position of the Fermi level on a freshly evaporated Au film. The position of the vacuum level, E_{vac}, was measured for each surface using the onset of the secondary cutoff in the UPS spectra. The HOMO/LUMO level was determined directly using the onset edge in the UPS/IPES spectra instead of the peak value. All measurements were performed at room temperature.

Synthesis Details for All New Compounds. General Procedure for the Coupling of a Terminal Alkyne with an Aryl Halide Using a Palladium-Catalyzed Cross-Coupling (Sonogashira) Protocol. To an oven-dried round-bottom flask equipped with a magnetic stir bar were added the aryl halide, the terminal alkyne, $PdCl_2(PPh_3)_2$ (ca. 2 mol % per aryl halide), and CuI (ca. 4 mol % per aryl halide). A solvent system of TEA and/or THF was added depending on the substrates. Upon completion, the reaction was quenched with a saturated solution of NH_4Cl. The organic layer was then diluted with hexanes, diethyl ether, or CH_2Cl_2 and washed with water or saturated NH_4Cl (1×). The combined aqueous layers were extracted with hexanes, diethyl ether, or CH_2Cl_2 (2×). The combined organic layers were dried over $MgSO_4$ and filtered, and the solvent was removed from the filtrate in vacuo to afford the crude product, which was purified

(38) Ying, J. W.; Ren, T. *J. Organomet. Chem.* **2006**, *691*, 4021–4027.
(39) Flatt, A. K.; Chen, B.; Taylor, P. G.; Chen, M. X.; Tour, J. M. *Chem. Mater.* **2006**, *18*, 4513–4518.
(40) He, T.; Ding, H. J.; Peor, N.; Lu, M.; Corley, D. A.; Chen, B.; Ofir, Y.; Gao, Y. L.; Yitzchaik, S.; Tour, J. M. *J. Am. Chem. Soc.* **2008**, *130*, 1699–1710.
(41) Yan, L.; Watkins, N. J.; Zorba, S.; Gao, Y. L.; Tang, C. W. *Appl. Phys. Lett.* **2001**, *79*, 4148–4150.
(42) Ding, H. J.; Zorba, S.; Gao, Y. L.; Ma, L. P.; Yang, Y. *J. Appl. Phys.* **2006**, *100*, 113706.

by column chromatography (silica gel). Eluents and other slight modifications are described below for each compound.

General Procedure for the Addition of C_{60} to Terminal Alkynes Using LHMDS, in Situ Ethynylation Method. To an oven-dried round-bottom flask equipped with a magnetic stir bar was added the terminal alkyne and C_{60} (2 equiv per terminal alkyne H). After addition of THF, the mixture was bath-sonicated for at least 3 h. To the greenish-brown suspension formed after the sonication was added LHMDS dropwise at room temperature over 0.5 to 1.5 h. As the reaction progressed, the mixture turned into a deep greenish-black solution. During and after the addition of the LHMDS, small aliquots from the reaction were extracted and quenched with trifluoroacetic acid (TFA) or methyl iodide (MeI), dried, and redissolved in CS_2 for TLC analysis (developed in a mixture of CS_2, CH_2Cl_2, and hexanes). Completion of the reaction was confirmed by the disappearance of the starting materials. The reaction usually completed within 1.5 h from the beginning of LHMDS addition. Upon completion, the reaction was quenched with TFA or MeI to give a brownish slurry. When MeI was used, the reaction was stirred at room temperature for at least 6 h. Excess TFA or MeI and solvent were then removed in vacuo to afford a crude product that was purified by flash column chromatography (silica gel). Eluents and other slight modifications are described below for each compound.

Compound 1-H-TMS. Compound **13** (0.080 g, 0.34 mmol) was subjected to the general in situ ethynylation procedure with C_{60} (0.12 g, 0.17 mmol), THF (100 mL), LHMDS (0.5 mL, 0.5 mmol), and TFA (0.23 mL). Crude products were dissolved in CS_2, directly loaded onto a flash column, and eluted with 7−20% CS_2 in hexanes. The product was further purified using another flash column with graduated elution of 50−100% CS_2 in hexanes to afford the product (0.086 g, 54%) as a brown solid: FTIR (KBr) 2945, 1488, 1246, 1092, 838 cm^{-1}; ^1H NMR (CS_2/$CDCl_3$, 1:1, 500 MHz) δ 7.66 (d, J = 8.4 Hz, 2H), 7.31 (d, J = 8.4 Hz, 2H), 7.11 (s, 1H), 3.04−3.01 (m, 2H), 1.02−0.98 (m, 2H), 0.10 (s, 9H); ^{13}C NMR (CS_2/$CDCl_3$, 1:1, 125 MHz) δ 151.5, 151.3, 147.6, 147.3, 146.6, 146.4, 146.3, 146.19, 146.17, 145.8, 145.63, 145.61, 145.5, 145.4, 145.3, 144.7, 144.5, 143.2, 142.6, 142.5, 142.1, 142.01, 141.97, 141.9, 141.7, 141.6, 140.4, 140.3, 136.1, 135.1 (30 signals from sp^2-C in the C_{60} core), 139.7, 132.3, 127.6, 118.9, 92.4, 83.6, 61.9 (*C*H in the C_{60} core), 55.1 (quaternary sp^3-C in the C_{60} core), 28.8, 16.6, −1.7; MALDI-TOF MS m/z (sulfur as the matrix) calcd for $C_{73}H_{18}SSi$ 955.1, found 955.0 (M^+).

Compound 2-H-TMS. Compound **16a** (0.094 g, 0.28 mmol) was subjected to the general in situ ethynylation procedure with C_{60} (0.13 g, 0.18 mmol), THF (100 mL), LHMDS (0.65 mL, 0.65 mmol), and TFA (0.1 mL, 1.3 mmol). Crude products were dissolved in CS_2, directly loaded onto a flash column, and eluted with 100% CS_2 in hexanes. The product was further purified using another flash column with graduated elution of 5−50% CS_2 in hexanes then CS_2/CH_2Cl_2/hexanes (3:1:6) to afford the product (0.061 g, 21%) as a brown solid: FTIR (KBr) 2945, 1507, 1246, 1086 cm^{-1}; ^1H NMR (CS_2/$CDCl_3$, 1:2, 500 MHz) δ 7.78 (d, J = 8.2 Hz, 2H), 7.61 (d, J = 8.1 Hz, 2H), 7.44 (d, J = 8.2 Hz, 2H), 7.24 (d, J = 8.2 Hz, 2H), 7.16 (s, 1H), 3.03−3.00 (m, 2H), 1.02−0.92 (m, 2H), 0.12 (s, 9H); ^{13}C NMR (CS_2/$CDCl_3$, 1:2, 125 MHz) δ 151.5, 151.2, 147.7, 147.4, 146.7, 146.53, 146.50, 146.34, 146.33, 145.9, 145.8, 145.7, 145.62, 145.55, 145.47, 144.8, 144.6, 143.3, 142.73, 142.70, 142.23, 142.17, 142.1, 142.0, 141.8, 141.7, 140.52, 140.49, 139.2 (Ar), 136.2, 135.3 (30 signals from sp^2-C in the C_{60} core), 132.2, 132.0, 131.7, 127.7, 124.3, 122.2, 119.7, 94.2, 92.2, 89.6, 83.7, 62.0 (*C*H in the C_{60} core), 55.3 (quaternary sp^3-C in the C_{60} core), 29.0, 16.8, −1.6; MALDI-TOF MS m/z (sulfur as the matrix) calcd for $C_{81}H_{22}SSi$ 1055.2, found 1056.4 (M^+).

Compound 3-Me-TMS. Compound **16b** (0.15 g, 0.40 mmol) was subjected to the general in situ ethynylation procedure with C_{60} (0.22 g, 0.31 mmol), THF (120 mL), LHMDS (1.0 mL, 1.0 mmol), and MeI (5 mL, 80 mmol). Crude products were dissolved in CS_2, directly loaded onto flash column, and eluted with 100% CS_2 in hexanes. The product was further purified using another flash column with graduated elution of 5−75% CS_2 in hexanes and then CS_2/CH_2Cl_2/hexanes (4:1:5) to afford the product (0.079 g, 23%) as a brown solid: FTIR (KBr) 2950, 2922, 2208, 1713, 1606, 1588, 1541, 1514, 1344, 1248 cm^{-1} (drop cast); ^1H NMR (CS_2/$CDCl_3$, 1:5, 500 MHz) δ 8.47 (d, J = 1.5 Hz, 1H), 7.95 (dd, J = 1.5, 8.3 Hz, 1H), 7.78 (d, J = 8.3 Hz, 1H), 7.51 (d, J = 8.6 Hz, 2H), 7.26 (d, J = 8.6 Hz, 2H), 3.52 (s, 3H), 3.03−2.99 (m, 2H), 0.99−0.96 (m, 2H), 0.08 (s, 9H); ^{13}C NMR (CS_2:$CDCl_3$, 1:5, 125 MHz) δ 156.6, 152.6, 149.4 (Ar), 148.0, 147.8, 146.6, 146.5, 146.4, 146.3, 145.9, 145.7, 145.6, 145.5, 145.4, 145.01, 144.98, 144.8, 144.6, 143.2, 142.71, 142.66, 142.21, 142.16, 142.1, 142.0, 141.7, 141.6, 140.7 (Ar), 140.4, 140.2, 135.7, 134.7 (30 signals from sp^2-C in the C_{60} core), 134.5, 134.2, 132.4, 128.2, 127.3, 123.1, 119.1, 118.5, 99.8, 92.6, 85.2, 82.8, 61.7 (*C*CH_3 in the C_{60} core), 59.7 (quaternary sp^3-C in the C_{60} core), 33.0, 28.6, 16.6, −1.7; MALDI-TOF MS m/z (sulfur as the matrix) calcd for $C_{82}H_{23}NO_2SSi$ 1114.2, found 1114.2 (M^+).

Compound 3-H-TMS. Compound **16b** (0.091 g, 0.24 mmol) was subjected to the general in situ ethynylation procedure with C_{60} (0.12 g, 0.16 mmol), THF (100 mL), LHMDS (1.8 mL, 1.8 mmol), and TFA (0.9 mL, 11.7 mmol). Crude products were dissolved in CS_2, directly loaded onto flash column, and eluted with 100% CS_2 in hexanes then CS_2/CH_2Cl_2/hexanes (6:1:3) to afford the product (0.055 g, 31%) as a brown solid: FTIR (KBr) 2945, 2204, 1540, 1521, 1498, 1342, 1246, 1087 cm^{-1}; ^1H NMR (CS_2:$CDCl_3$, 1:1, 500 MHz) δ 8.49 (d, J = 1.7 Hz, 1H), 7.96 (dd, J = 8.0, 1.7 Hz, 1H), 7.77 (d, J = 8.0 Hz, 1H), 7.49 (d, J = 6.6 Hz, 2H), 7.22 (d, J = 6.6 Hz 2H), 7.12 (s, 1H), 3.01−2.97 (m, 2H), 0.99−0.95 (m, 2H), 0.09 (s, 9H); ^{13}C NMR (CS_2:$CDCl_3$, 1:1, 125 MHz) δ 151.0, 150.3, 149.3 (Ar), 147.6, 147.3, 146.5, 146.44, 146.38, 146.24, 146.23, 145.8, 145.7, 145.51, 145.46, 145.42, 145.35, 144.7, 144.4, 143.2, 142.64, 142.60, 142.1, 142.05, 141.99, 141.74, 141.69, 141.64, 140.8 (Ar), 140.43, 140.41, 135.9, 135.5 (Ar), 135.3 (30 signals from sp^2-C in the C_{60} core), 134.4, 132.3, 128.3, 127.2, 122.8, 119.2, 118.5, 100.0, 96.2, 85.3, 81.2, 61.5 (*C*H in the C_{60} core), 55.0 (quaternary sp^3-C in the C_{60} core), 28.6, 16.6, −1.8; MALDI-TOF MS m/z (sulfur as the matrix) calcd for $C_{81}H_{21}NO_2SSi$ 1100.2, found 1101.2 (M^+).

Compound 4-TMS. Compound **16c** (0.100 g, 0.275 mmol) was subjected to the general in situ ethynylation procedure with C_{60} (0.297 g, 0.413 mmol), THF (125 mL), LHMDS (0.600 mL, 0.600 mmol), and MeI (6 mL). Crude products were dissolved in CS_2, directly loaded onto flash column, and eluted with 1−40% CS_2 in hexanes. The product was further purified using another flash column with graduated elution from hexanes to CS_2/CH_2Cl_2/hexanes (1:3:6) to afford the product (0.093 g, 31%) as a brown solid: FTIR (KBr) 2960, 1496, 1429, 1248 cm^{-1}; ^1H NMR (CS_2/$CDCl_3$, 1:5, 400 MHz) δ 7.65 (s, 1H), 7.59 (m, 2H), 7.46 (d, J = 8.1 Hz, 2H), 7.28 (s, 1H), 3.53 (s, 3H), 2.99 (m, 4H), 1.39 (t, J = 7.5 Hz, 3H), 0.97 (m, 2H), 0.07 (s, 9H); ^{13}C NMR (CS_2:$CDCl_3$, 1:5, 100 MHz) δ 157.1, 153.4, 148.0, 147.8, 146.6, 146.5, 146.4, 146.3, 146.0, 145.61, 145.56, 145.5, 145.4, 145.3, 145.1, 144.8, 144.7, 143.2, 143.1, 142.6, 142.2, 142.1, 142.0, 141.7, 141.6, 140.3, 140.2, 138.7, 134.6, 134.4, 132.2, 131.9, 311.8, 131.76, 131.6, 129.4, 128.0, 123.2, 122.4, 120.0, 94.9, 89.5, 88.1, 85.4, 61.8, 59.9, 33.0, 29.0, 27.8, 16.7, 14.7, −1.7; MALDI-TOF MS m/z (sulfur as the matrix) calcd for $C_{84}H_{28}SSi$ 1096, found 1096 (M^+).

Compound 4-SAc. To a round-bottom flask equipped with a magnetic stirrer were added compound **4-TMS** (32 mg, 0. 029 mmol), excess AcCl (1 mL), CH_2Cl_2 (20 mL), and $AgBF_4$ (17 mg, 0.08 mmol). The reaction mixture was stirred for 1 h at room temperature and then quenched with saturated $NaHCO_3$ and

diluted with CH_2Cl_2 and water. The aqueous layer was extracted with CH_2Cl_2 (×1). The combined organic layers were dried over $MgSO_4$, filtered, and concentrated under vacuum. Crude material was loaded onto flash column using pure CS_2 and eluted with hexane, CS_2/CH_2Cl_2/hexane (1:1:3), and then CS_2/CH_2Cl_2/hexane (5:2:3) to give the product **4-SAc** as a brown powder (12.0 mg, 40%): FTIR (KBr) 2963, 2923, 1709, 1495 cm^{-1}; ^1H NMR ($CS_2/CDCl_3$, 1:1, 400 MHz) δ 7.64 (m, 1H), 7.57 (m, 4H), 7.41 (d, $J = 8$ Hz, 2H), 3.53 (s, 3H), 2.96 (q, $J = 8$ Hz, 2H), 2.45 (s, 3H), 1.39 (t, $J = 8$ Hz, 3H); ^{13}C NMR ($CS_2/CDCl_3$, 1:1, 100 MHz) δ 157.0, 153.2, 147.9, 147.7, 146.52, 146.51, 146.4, 146.3, 146.2, 146.0, 145.6, 145.5, 145.4, 145.3, 145.2, 145.0, 144.8, 144.7, 143.2, 142.7, 142.6, 142.2, 142.13, 142.12, 142.0, 141.7, 141.5, 140.3, 140.2, 134.5, 134.4, 134.2, 132.3, 132.0, 131.6, 129.4, 128.4, 124.4, 122.8, 122.7, 94.2, 89.7, 89.6, 85.3, 61.7, 59.8, 33.0, 30.2, 29.9, 27.9, 14.8; MALDI-TOF MS m/z (sulfur as the matrix) calcd for $C_{81}H_{18}OS$ 1038, found 1038 (M^+).

Compound 5-TMS. Compound **16d** (0.130 g, 0.322 mmol) was subjected to the general in situ ethynylation procedure with C_{60} (0.255 g, 0.354 mmol), THF (120 mL), LHMDS (3.217 mL, 3.217 mmol), and MeI (6 mL). Crude products were dissolved in CS_2, directly loaded onto flash column, and eluted with CS_2. The product was further purified using another flash column with graduated elution from hexanes/CS_2 (1:1) to afford the product (0.163 g, 45%) as a brown solid: FTIR (KBr) 2959, 2919, 2855, 2226, 1499, 1420, 1322, 1254, 1171, 1134, 1046, 908, 843, 727 cm^{-1}; ^1H NMR ($CDCl_3$, 500 MHz) δ 8.08 (d, 1H, $J =$ 1.15 Hz), 7.91 (dd, 1H, $J = 1.56$ Hz, $J = 7.93$ Hz), 7.75 (d, 1H, $J =$ 7.97 Hz), 7.49 (td, 1H, $J = 2.18$ Hz, $J = 8.20$ Hz), 7.28 (td, 1H, $J =$ 2.00 Hz, $J = 8.31$ Hz), 3.53 (s, 3H), 3.01 (m, 2H), 0.96 (m, 2H), 0.07 (s, 9H); ^{13}C NMR ($CDCl_3$), 125 MHz) δ 156.89, 152.95, 148.01, 147.8, 146.64, 146.54, 146.41, 146.37, 146.02, 145.70, 145.63, 145.54, 145.43, 145.15, 145.10, 144.85, 144.71, 143.28, 143.12, 142.74, 142.69, 142.26, 142.21, 142.19, 142.04, 141.73, 141.60, 140.40, 140.27, (30 signals from sp^2-C in the C_{60} core), 139.83, 134.75 134.72, 134.35, 133.82, 132.08, 129.68, 129.64, 127.60, 124.34. 122.37, 119.01, 97.30, 91.57, 85.51, 83.72, 61.77 (CCH_3 in the C_{60} core), 59.81 (quaternary sp^3-C in the C_{60} core), 33.09, 28.78, 16.64, −1.70; MALDI-TOF MS m/z (CHCA as the matrix) calcd for $C_{83}H_{23}F_3SSi$ 1136, found 1137 (M^+).

Compound 5-SAc. To a round-bottom flask equipped with a magnetic stirrer were added compound **5** (0.050 mg, 0.045 mmol), excess AcCl (1 mL), CH_2Cl_2 (20 mL), and $AgBF_4$ (0.026 mg, 0.134 mmol). The reaction mixture was stirred for 1 h at room temperature and then quenched with saturated $NaHCO_3$ and diluted with CH_2Cl_2 and water. The aqueous layer was extracted with CH_2Cl_2 (×1). The combined organic layers were dried over $MgSO_4$, filtered, and concentrated under vacuum. Crude material was loaded onto flash column using pure CS_2 and eluted with hexane and then CS_2/CH_2Cl_2/hexane (5:2:3) to give the product as a brown powder (33.5 mg, 70%): FTIR (KBr) 2919, 2843, 2216, 1706, 1506, 1418, 1318, 1170, 1129, 1049, 828 cm^{-1}; ^1H NMR ($CS_2/CDCl_3$, 1:1, 500 MHz) δ 8.11 (d, 1H, $J = 0.91$ Hz), 7.94 (dd, 1H, $J = 1.39$ Hz, $J = 7.77$ Hz), 7.78 (d, 1H, $J = 7.93$ Hz), 7.63 (td, 2H, $J = 1.88$ Hz, $J = 8.40$ Hz) 7.46 (td, 2H, $J = 1.64$ Hz, $J = 8.24$ Hz), 3.54 (s, 3H), 2.47 (s, 3H); ^{13}C NMR ($CS_2/CDCl_3$, 1:1, 125 MHz) δ; 156.87, 152.91, 148.01, 147.85, 146.65, 146.54, 146.41, 146.37, 146.02, 145.71, 145.63, 145.54, 145.43, 145.14, 145.10, 144.85, 144.71, 143.28, 143.26, 142.74, 142.70, 142.26, 142.21, 142.19, 142.03, 141.73, 141.60, 140.41, 140.27, 139.67, 134.78 (30 signals from sp^2-C in the C_{60} core), 134.73, 134.34, 134.02, 132.35, 129.66, 129.20, 126.94, 123.62, 122.86, 119.74, 96.15, 91.81, 85.19, 83.62, 61.77 (CCH_3 in the C_{60} core), 59.80 (quaternary sp^3-C in the C_{60} core), 33.09, 29.75; MALDI-TOF MS m/z (CHCA as the matrix) calcd for $C_{80}H_{13}F_3OS$ 1078, found 1079 (M^+).

Compound 6-TMS. Compound **16e** (100 mg, 0.222 mmol) was subjected to the general in situ ethynylation procedure with C_{60} (240 mg, 0.333 mmol), THF (120 mL), LHMDS (0.6 mL, 0.6 mmol), and MeI (1 mL). Crude products were dissolved in CS_2, directly loaded onto a flash column, and eluted with 1−40% CS_2 in hexanes. The product was further purified using another flash column with gradual elution from hexanes to CS_2/CH_2Cl_2/hexanes (5:1:4) to afford the product (80 mg, 30%) as a brown solid: FTIR (KBr) 2925, 2854, 1742, 1443, 144, 1377, 1259, 1213, 1097, 859 cm^{-1}; ^1H NMR ($CDCl_3$, 500 MHz) δ 7.47 (d, 2H, $J = 8.19$ Hz), 7.26 (d, 2H, $J = 8.19$ Hz), 7.20 (s, 1H), 7.10 (s, 1H), 4.10 (t, 2H, $J = 6.40$ Hz), 4.07 (t, 2H, $J = 6.40$ Hz), 3.56 (s, 3H), 3.00 (m, 2H), 1.94 (m, 4H), 1.16 (t, 3H, $J = 7.40$ Hz), 1.13 (t, 3H, $J = 7.40$ Hz), 0.96 (m, 2H), 0.07 (s, 9H); ^{13}C NMR ($CDCl_3$), 126 MHz) δ 157.3, 154.7, 153.59, 153.56, 148.0, 147.8, 146.56, 146.48, 146.34, 146.30, 146.03, 145.58, 145.55, 145.49, 145.38, 145.36, 145.2, 144.8, 144.7, 143.2, 142.67, 142.63, 142.22, 142.16, 142.13, 141.7, 141.5, 140.3, 140.2, 138.6, 134.6, 134.5, 131.9, 127.8, 120.2, 117.4, 116.3, 114.8, 113.0, 95.1, 93.5, 86.3, 82.0, 71.4, 70.9, 61.8, 60.2, 33.3, 29.0, 23.0, 22.9, 16.7, 10.9, 10.8, −1.7; MALDI-TOF MS m/z (sulfur as the matrix) calcd for $C_{88}H_{36}SSi$ 1185, found 1185 (M^+).

Compound 6-SAc. To a round-bottom flask equipped with a magnetic stirrer were added compound **6-TMS** (50 mg, 0.042 mmol), excess AcCl (1 mL), CH_2Cl_2 (20 mL), and $AgBF_4$ (25 mg, 0.128 mmol). The reaction mixture was stirred for 1 h at room temperature and then quenched with saturated $NaHCO_3$ and diluted with CH_2Cl_2 and water. The aqueous layer was extracted with CH_2Cl_2 (×1). The combined organic layers were dried over $MgSO_4$, filtered, and concentrated under vacuum. Crude material was loaded onto flash column using pure CS_2 and eluted with hexane, CS_2/CH_2Cl_2/hexane (1:1:3), and then CS_2/CH_2Cl_2/hexane (5:2:3) to give the product as a brown powder (11 mg, 24%): FTIR (KBr) 2923, 1716, 1626, 1383, 1181 cm^{-1}; ^1H NMR ($CDCl_3$, 500 MHz) δ 7.59 (d, 2H, $J =$ 8.19 Hz), 7.42 (d, 2H, $J = 8.19$ Hz), 7.22 (s, 1H), 7.12 (s, 1H), 4.12 (t, 2H, $J = 6.40$ Hz), 4.08 (t, 2H, $J = 6.40$ Hz), 3.57 (s, 3H), 2.45 (s, 3H), 1.98 (m, 2H), 1.91 (m, 2H), 1.19 (t, 3H, $J = 7.40$ Hz), 1.14 (t, 3H, $J = 7.40$ Hz); ^{13}C NMR ($CDCl_3$, 125 MHz) δ 157.25, 154.65, 153.53, 153.50, 147.90, 147.74, 146.50, 146.43, 146.28, 146.24, 145.97, 145.52, 145.49, 145.43, 145.32, 145.30, 145.13, 144.76, 144.67, 143.17, 142.61, 142.57, 142.16, 142.10, 142.07, 141.63, 141.48, 140.24, 140.14, 138.51, 134.57, 134.41, 131.86, 127.73, 120.12, 117.35, 116.25, 114.73, 112.91, 95.04, 93.48, 86.19, 81.97, 71.29, 70.86, 61.76, 60.17, 33.26, 22.97, 22.82, 10.87, 10.70; MALDI-TOF MS m/z (sulfur as the matrix) calcd for $C_{85}H_{26}OS$ 1126, found 1127 ($M + H^+$).

Compound 7. Compound **13** (0.086 g, 0.37 mmol) was subjected to the general in situ ethynylation procedure with C_{60} (0.22 g, 0.31 mmol), THF (120 mL), LHMDS (0.6 mL, 0.6 mmol), and $C_7H_{15}I$ (10 mL, 60 mmol). Crude products were dissolved in CS_2, directly loaded onto flash column, and eluted with 100% CS_2 in hexanes. The product was further purified using another flash column with graduated elution of 5−50% CS_2 in hexanes to afford the product (0.022 g, 7%) as a brown solid: FTIR (KBr) 2947, 2920, 2849, 1711, 1489, 1461, 1429, 1247, 1088 cm^{-1}; ^1H NMR ($CDCl_3$, 500 MHz) δ 7.68 (d, $J = 8.4$ Hz, 2H), 7.36 (d, $J = 8.4$ Hz, 2H), 3.78−3.74 (m, 2H), 3.07−3.04 (m, 2H), 2.62 (m, 2H), 1.81 (m, 2H), 1.59−1.55 (m, 2H), 1.42−1.38 (m, 4H), 1.02−1.01 (m, 2H), 1.00 (t, $J = 4.1$ Hz, 3H), 0.10 (s, 9H); ^{13}C NMR ($CDCl_3$, 125 MHz) δ 156.1, 154.1, 147.9, 147.8, 146.6, 146.5, 146.33, 146.31, 146.0, 145.8, 145.57, 145.55, 145.5, 145.4, 145.3, 144.8, 144.7, 143.3, 142.69, 142.66, 142.237 (× 2), 142.13, 142.11, 141.7, 141.5, 140.3, 139.9, 134.9, 134.5 (30 signals from sp^2-C in the C_{60} core), 139.2, 132.4, 127.9, 119.4, 89.2, 84.3, 66.1 (CCH_3 in the C_{60} core), 59.8 (quaternary sp^3-C in the C_{60} core), 44.6, 32.0, 30.7, 30.4, 29.6, 28.9, 22.7, 16.7, 14.2, −1.66; MALDI-TOF MS m/z (sulfur as the matrix) calcd for $C_{80}H_{32}SSi$ 1053.3 (unable to obtain mass due to instability of molecular ion).

Compound 11. To a round-bottom flask equipped with a magnetic stirrer were added **34** (36 mg, 0.018 mmol), CH_2Cl_2

(10 mL), and $AgBF_4$ (10−20 mg, 0.05−0.1 mmol). The reaction mixture was stirred for 0.5 h at room temperature and then quenched with saturated $NaHCO_3$ and diluted with CH_2Cl_2 and water. The aqueous layer was extracted with CH_2Cl_2 (×2). The combined organic layers were dried over $MgSO_4$, filtered, and concentrated under vacuum. Crude material was loaded onto flash column using pure CS_2 and eluted with hexane, CS_2/CH_2Cl_2/hexane (2:4:4), CS_2/CH_2Cl_2/hexane (2:5:3), CS_2/CH_2Cl_2/hexane (2:6:2), and then CS_2/CH_2Cl_2/hexane (1:7:2) to give the product **11** as brown solid (21.7 mg, 66%): FTIR (KBr) 2920, 1688, 1594, 1130, 1098 cm^{-1}; ^1H NMR ($CDCl_3$, 500 MHz) δ 8.05 (d, J = 8.5 Hz, 2H), 7.99 (d, J = 8.4 Hz, 2H), 7.95 (d, J = 8.6 Hz, 2H), 7.73 (d, J = 8.5 Hz, 2H), 7.62−7.53 (m, 16H), 7.49 (m, 3H), 7.44−7.42 (m, 3H), 7.31−7.28 (m, 6H), 4.12 (s, 6H), 3.56 (s, 3H), 2.37 (s, 9H); ^{13}C NMR ($CDCl_3$, 125 MHz) δ 194.9 (Ac), 157.0, 153.2, 152.2 (Ar), 151.9 (Ar), 148.0, 147.8, 146.6, 146.5, 146.4, 146.3, 146.0, 145.64, 145.58, 145.5, 145.4, 145.2, 145.1, 144.8, 144.7, 143.2, 142.70, 142.66, 142.23, 142.173 (× 2), 142.1, 141.7, 141.6, 140.3, 140.2, 138.0 (Ar), 136.3 (Ar), 136.2 (Ar), 134.7, 134.4 (30 signals from sp^2-C in the C_{60} core), 134.1, 133.5, 133.0, 132.6, 132.0, 131.14, 131.09, 130.6, 129.0, 128.7, 126.2, 125.5, 124.9, 124.5, 123.4, 123.24, 123.16, 96.1, 92.1, 91.0, 90.5, 89.4, 85.0, 61.8 (CCH_3 in the C_{60} core), 59.9 (quaternary sp^3-C in the C_{60} core), 33.1, 30.4, 29.7; MALDI-TOF MS m/z (sulfur as the matrix) calcd for $C_{134}H_{54}N_2O_3S_3Si$ 1864.2 (unable to obtain mass due to instability of molecular ion).

Compound 12. Compound **35** (0.13 g, 0.65 mmol) was subjected to the general in situ ethynylation procedure with C_{60} (0.22 g, 0.30 mmol), THF (100 mL), LHMDS (1.0 mL, 1.0 mmol), and MeI (6.0 mL, 96 mmol). Crude products were dissolved in CS_2, directly loaded onto a flash column, and purified with gradual elution of 1−50% CS_2 in hexanes to afford the product **12** (0.15 g, 52%) as a brown solid: FTIR (KBr) 2968, 2922, 2864, 1712, 1421, 1391, 1325, 1229, 1072 cm^{-1}; ^1H NMR (CS_2:$CDCl_3$ (1:5), 500 MHz) δ 7.69 (d, J = 8.1 Hz, 2H), 7.47 (d, J = 8.1 Hz, 2H), 3.81 (q, J = 7.2 Hz, 4H), 3.53 (s, 3H), 1.32 (m, 6H); ^{13}C NMR (CS_2:$CDCl_3$ (1:5), 125 MHz) δ 157.2, 153.7, 151.4 (Ar), 147.9, 147.7, 146.5, 146.4, 146.3, 146.2, 146.0, 145.52, 145.47, 145.4, 145.32, 145.29, 145.1, 144.74, 144.69, 143.2, 142.59, 142.57, 142.2, 142.14, 142.10, 142.09, 141.6, 141.5, 140.22, 140.16, 134.45, 134.42 (30 signals from sp^2-C in the C_{60} core), 132.7, 120.6, 118.7, 87.7, 86.1, 61.7 (CCH_3 in the C_{60} core), 59.8 (quaternary sp^3-C in the C_{60} core), 33.0; MALDI-TOF MS m/z (sulfur as the matrix) calcd for $C_{73}H_{17}H_3$ 935.9, found 936.6 (M^+).

Compound 15b. See the general procedure for the Pd/Cu coupling reaction. The materials used were **14b** (1.03 g, 2.98 mmol), **13** (0.615 g, 2.62 mmol), $PdCl_2(PPh_3)_2$ (0.033 g, 0.047 mmol), CuI (0.014 g, 0.074 mmol), TEA (10 mL), and THF (20 mL) at room temperature overnight. The residue was purified by flash column chromatography with 10−20% CH_2Cl_2 in hexanes to give product **15b** (0.99 g, 84%) as a yellow solid: FTIR (KBr) 2954, 2211, 2163, 1588, 1542, 1499, 1346, 1249, 1089 cm^{-1}; ^1H NMR (500 MHz, $CDCl_3$) δ 8.16 (s, 1H), 7.63 (s, 2H), 7.49 (d, J = 8.5 Hz, 2H), 7.26 (d, J = 8.5 Hz, 2H), 3.03−2.98 (m, 2H), 0.99−0.94 (m, 2H), 0.28 (s, 9H), 0.07 (s, 9H); ^{13}C NMR (125 MHz, $CDCl_3$) δ 149.4, 140.6, 135.8, 134.5, 132.5, 128.3, 127.6, 123.9, 118.9, 118.7, 102.2, 99.6, 99.3, 85.3, 28.8, 16.8, −0.1, −1.5; EI-HRMS m/z calcd for $C_{24}H_{29}NO_2SSi_2$ 451.14, found 452.15 ($[M + H]^+$).

Compound 16b. To a round-bottom flask equipped with a magnetic stirrer were added **15b** (0.36 g, 0.8 mmol), THF/MeOH (1:1) (30 mL), and K_2CO_3 (0.16 g, 1.2 mmol). The reaction mixture was stirred for 1 h at room temperature and then quenched with water and diluted with hexanes. The aqueous layer was extracted with CH_2Cl_2 (×2). The combined organic layers were dried over $MgSO_4$, filtered, and concentrated under vacuum. Crude material was filtered through a plug of silica gel using CH_2Cl_2/hexanes mixture to give the product **16b** as a reddish-brown solid (0.30 g, 99%): FTIR (KBr) 3288, 2951, 2209, 1588, 1498 cm^{-1}; ^1H NMR (400 MHz, $CDCl_3$) δ 8.19(s, 1H), 7.66 (s, 2H), 7.50 (d, J = 6.7 Hz, 2H), 7.26 (d, J = 6.7 Hz, 2H), 3.30 (s, 1H), 3.03−2.99 (m, 2H), 0.99−0.94 (m, 2H), 0.08 (s, 9H); ^{13}C NMR (100 MHz, $CDCl_3$) δ 149.4, 140.7, 136.0, 134.6, 132.6, 128.5, 127.6, 122.8, 119.2, 118.8, 99.5, 85.1, 81.5, 81.2, 28.8, 16.8, −1.5; EI-HRMS m/z calcd for $C_{21}H_{21}NO_2SSi$ 379.1062, found 380.11362 ($[M + H]^+$).

Compound 16c. See the general procedure for the Pd/Cu coupling reaction. The materials used were **14c** (0.353 g, 1.506 mmol), **13** (0.498 g, 1.506 mmol), $PdCl_2(PPh_3)_2$ (0.025 g, 0.036 mmol), CuI (0.010 g, 0.053 mmol), TEA (10 mL), and THF (20 mL) at room temperature overnight. The residue was purified by flash column chromatography with 1−5% CH_2Cl_2 in hexanes to give product **15c** (0.471 g, 72%) as a yellow oil. The solid was then transferred to a round-bottom flask equipped with a magnetic stirrer dissolved in THF/MeOH (1:1) (30 mL) and K_2CO_3 (0.312 g, 2.26 mmol). The reaction mixture was stirred for 1 h at room temperature and then quenched with water and diluted with hexanes. The aqueous layer was extracted with CH_2Cl_2 (×1). The combined organic layers were dried over $MgSO_4$, filtered, and concentrated under vacuum. The crude material was filtered through a plug of silica gel using CH_2Cl_2/hexanes (20%) mixture to give the product **16c** as yellow/orange oil (0.372 g, 99%): FTIR (KBr) 3294, 2952, 1590, 1496, 1248 cm^{-1}; ^1H NMR (400 MHz, $CDCl_3$) δ 7.37 (m, 3H), 7.32 (d, J = 1 Hz, 1H), 7.24 (dd, J_1 = 8 Hz, J_2 = 1.5 Hz, 1H), 7.19 (d, J = 8.5 Hz, 2H), 3.09 (s, 1H), 2.95 (m, 2H), 2.8 (q, J = 7.5 Hz, 2H), 1.23 (t, J = 7.5 Hz, 3H), 0.88 (m, 2H), 0.00 (s, 9H); ^{13}C NMR (100 MHz, $CDCl_3$) δ 146.2, 138.8, 132.1, 132.0, 131.8, 129.5, 128.0, 123.3, 122.0, 120.1, 94.8, 88.1, 83.8, 78.6, 29.1, 27.7, 16.8, 14.7, −1.6; EI-HRMS m/z calcd for $C_{23}H_{26}SSi$ 362.1524, found 362.1525.

Compound 16d. See the general procedure for the Pd/Cu coupling reaction. The materials used were **14d** (0.269 g, 1.145 mmol), **13** (0.422 g, 1.145 mmol), $PdCl_2(PPh_3)_2$ (0.025 g, 0.036 mmol), CuI (0.010 g, 0.053 mmol), TEA (10 mL), and THF (20 mL) at room temperature overnight. The residue was purified by flash column chromatography with 1−5% CH_2Cl_2 in hexanes to give product **15d** (0.442 g, 81%) as a yellow oily solid. The solid was then transferred to a round-bottom flask equipped with a magnetic stirrer dissolved in THF/MeOH (1:1) (30 mL) and K_2CO_3 (0.237 g, 1.718 mmol). The reaction mixture was stirred for 1 h at room temperature and then quenched with water and diluted with hexanes. The aqueous layer was extracted with CH_2Cl_2 (×1). The combined organic layers were dried over $MgSO_4$, filtered, and concentrated under vacuum. The crude material was filtered through a plug of silica gel using CH_2Cl_2/hexanes (10%) mixture to give the product **16d** as a yellow shiny solid (0.360 g, 99%): FTIR (KBr) 3240, 2946, 2913, 2886, 2217, 1589, 1502, 1420, 1318, 1251, 1170, 1140, 1083, 1053, 824 cm^{-1}; ^1H NMR (500 MHz, $CDCl_3$) δ 7.80 (s, 1H), 7.61 (d, 2H, J = 1.17 Hz), 7.45 (td, 2H, J = 1.94 Hz, J = 8.66 Hz), 7.26 (td, 2H, J = 1.98 Hz, J = 8.57 Hz), 3.25 (s, 1H), 3.00 (m, 2H), 0.96 (m, 2H), 0.07 (s, 9H); ^{13}C NMR (125 MHz, $CDCl_3$) δ 139.7, 134.7, 133.6, 132.0, 131.8, 131.5, 129.74, 129.69, 129.63, 129.58, 127.6, 121.9, 119.0, 97.0, 85.3, 82.0, 80.3, 28.8, 16.7, −1.7; EI-HRMS m/z calcd for $C_{22}H_{21}F_3SSi$ 402.1084, found 402.1085.

Compound 16e. See the general procedure for the Pd/Cu coupling reaction. The materials used were **14e** (0.200 g, 0.853 mmol), **13** (0.328 g, 0.853 mmol), $PdCl_2(PPh_3)_2$ (0.030 g, 0.043 mmol), CuI (0.015 g, 0.079 mmol), TEA (10 mL), and THF (20 mL) at room temperature overnight. The residue was purified by flash column chromatography with 10% ethyl acetate in hexanes to give product **15e** (0.318 g, 76%) as a orange oil. The solid was then transferred to a round-bottom flask equipped with a magnetic stirrer dissolved in THF/MeOH (1:1) (30 mL) and K_2CO_3 (0.177 g, 1.280 mmol). The reaction mixture was stirred for 1 h at room temperature and then quenched with water and diluted with hexanes. The aqueous

layer was extracted with CH_2Cl_2 (×1). The combined organic layers were dried over $MgSO_4$, filtered, and concentrated under vacuum. The crude material was purified by flash column chromatography with 5% ethyl acetate in hexanes to give the product **16e** as a yellow/brown oily solid (0.261 g, 82%): FTIR (KBr) 3281, 2960, 2873, 2104, 1592, 1509, 1409, 1384, 1247, 1221, 1016, 861 cm^{-1}; ^1H NMR (400 MHz, $CDCl_3$) δ 7.42 (d, 2H, J = 8.28 Hz), 7.24 (d, 2H, J = 8.35 Hz), 6.98 (s, 1H), 6.97 (s, 1H), 3.97 (m, 4H), 3.34 (s, 1H), 3.01−2.96 (m, 2H), 1.90−1.80 (m, 4H), 1.11−1.04 (m, 6H), 0.97−0.92 (m, 2H), 0.05 (s, 9H); ^{13}C NMR (100 MHz, $CDCl_3$) δ 154.4, 153.6, 138.7, 132.1, 128.0, 120.3, 118.1, 117.0, 115.0, 113.7, 95.0, 86.2, 82.2, 80.2, 71.33, 71.30, 29.1, 22.9, 22.8, 16.8, 10.8, 10.7, −1.5; EI-HRMS m/z calcd for $C_{27}H_{34}O_2SSi$ 450.2049, found 450.2049.

Compound 32. See the general procedure for the Pd/Cu coupling reaction. The materials used were **30**[16] (0.456 g, 0.415 mmol), **31** (0.15 g, 0.37 mmol), $PdCl_2(PPh_3)_2$ (0.009 g, 0.012 mmol), CuI (0.003 g, 0.016 mmol), TEA (2 mL), and THF (10 mL) at room temperature overnight. The residue was purified by flash column chromatography with 5−33% CH_2Cl_2 in hexanes to give product **32** (0.28 g, 55%) as a clear red solid: FTIR (KBr) 3064, 2951, 2907, 2155, 1597, 1248, 1101 cm^{-1}; ^1H NMR (500 MHz, $CDCl_3$) δ 7.93 (d, J=8.7 Hz, 2H), 7.89 (d, J=8.7 Hz, 2H), 7.70 (d, J=8.7 Hz, 2H), 7.63−7.53 (m, 18H), 7.51 (m, 3H), 7.45−7.42 (m, 3H), 7.32−7.29 (m, 6H), 3.73 (s, 6H), 2.50−2.45 (m, 6H), 0.90−0.86 (m, 6H), 0.29 (s, 9H), 0.01 (s, 27H); ^{13}C NMR (125 MHz, $CDCl_3$) δ 152.13, 152.12, 139.2, 136.5, 136.4, 134.3, 133.7, 133.1, 132.8, 132.2, 131.34, 131.29, 130.4, 129.3, 128.8, 126.273 (× 2), 125.2, 124.8, 123.4, 123.3, 123.1, 104.8, 97.6, 92.1, 90.9, 90.8, 89.4, 35.9, 27.2, 17.2, 0.12, −1.5; MALDI-TOF MS m/z (sulfur as the matrix) calcd for $C_{85}H_{90}N_2S_3Si_5$ 1376.3 (unable to obtain mass due to instability of molecular ion).

Compound 33. To a round-bottom flask equipped with a magnetic stirrer were added **32** (0.17 g, 0.12 mmol), THF/MeOH (1:1) (20 mL), and K_2CO_3 (0.10 g, 0.72 mmol). The reaction mixture was stirred for 1 h at room temperature and then quenched with water and diluted with hexanes. The aqueous layer was extracted with CH_2Cl_2 (×2). Combined organic layers were dried over $MgSO_4$, filtered, and concentrated under vacuum. The residue was purified by flash column chromatography with 10−30% CH_2Cl_2 in hexanes to give product **33** (0.12 g, 76%) as a clear red solid: FTIR (KBr) 3289, 3064, 2923, 2852, 1597, 1247, 1101 cm^{-1}; ^1H NMR (400 MHz, $CDCl_3$) δ 7.95 (d, J=8.5 Hz, 2H), 7.91 (d, J= 8.5 Hz, 2H), 7.71 (d, J = 8.5 Hz, 2H), 7.66 (d, J = 8.5 Hz, 2H), 7.64−7.55 (m, 16H), 7.52 (m, 3H), 7.46−7.43 (m, 3H), 7.34−7.30 (m, 6H), 3.74 (s, 6H), 3.25 (s, 1H), 2.48 (m, 6H), 0.91−0.86 (m, 6H), 0.02 (s, 27H); ^{13}C NMR (100 MHz, $CDCl_3$) δ 152.4, 152.0, 139.2, 136.5, 136.4, 134.4, 133.7, 133.2, 132.8, 132.2, 131.34, 131.27, 130.4, 129.2, 128.7, 126.3, 125.18, 125.16, 124.8, 123.4, 123.3, 123.1, 92.2, 90.9, 90.7, 89.4, 83.5, 79.9, 35.9, 27.1, 17.2, −1.5; MALDI-TOF MS m/z (sulfur as the matrix) calcd for $C_{82}H_{82}N_2S_3Si_4$ 1304.1, found 1304.0 (M^+).

Compound 34. Compound **33** (0.17 g, 0.13 mmol) was subjected to the general in situ ethynylation procedure with C_{60} (0.11 g, 0.16 mmol), THF (290 mL), LHMDS (0.6 mL, 0.6 mmol), and MeI (2.5 mL, 40 mmol). Crude products were dissolved in CS_2, directly loaded onto the flash column, and purified with graduated elution of 1−40% CS_2 in hexanes then CS_2/CH_2Cl_2/hexanes (2:3:5) and CS_2/CH_2Cl_2/hexanes (1:4:5) to afford the product (0.057 g, 22%) as a brown solid: FTIR (KBr) 1703, 1595, 1360, 1248, 1221, 1097 cm^{-1}; ^1H NMR ($CDCl_3$, 500 MHz) δ 8.05 (d, J= 8.4 Hz, 2H), 7.99 (d, J=8.5 Hz, 2H), 7.95 (d, J=8.4 Hz, 2H), 7.73 (d, J=8.5 Hz, 2H), 7.62−7.54 (m, 16H), 7.50 (m, 3H), 7.44−7.42 (m, 3H), 7.32−7.29 (m, 6H), 3.72 (s, 6H), 3.56 (s, 3H), 2.48−2.45 (m, 6H), 0.89−0.85 (m, 6H), 0.003 (s, 27H); ^{13}C NMR ($CDCl_3$, 125 MHz) δ 157.0, 153.2, 152.2 (Ar), 151.9 (Ar), 148.0, 147.8, 146.6, 146.5, 146.4, 146.3, 146.0, 145.64, 145.59, 145.5, 145.4, 145.2, 145.1, 144.8, 144.7, 143.2, 142.69, 142.66, 142.23, 142.18, 142.175 (× 2), 141.7, 141.6, 140.3, 140.2, 139.0 (Ar), 136.3 (Ar), 136.2 (Ar), 134.7, 134.4 (30 signals from sp^2-C in the C_{60} core), 134.2, 133.5, 133.0, 132.6, 132.0, 131.14, 131.07, 130.2, 129.0, 128.5, 126.2, 125.5, 124.9, 124.5, 123.24, 123.16, 123.1, 96.1, 92.1, 91.0, 90.7, 89.2, 85.0, 61.8 ($C$$CH_3$ in the C_{60} core), 59.9 (quaternary sp^3-C in the C_{60} core), 35.6, 33.1, 26.9, 17.0, −1.8; MALDI-TOF MS m/z (sulfur as the matrix) calcd for $C_{143}H_{84}N_2S_3Si_4$ 2038.8 (unable to obtain mass due to instability of molecular ion).

Acknowledgment. The Welch Foundation, DARPA/AFOSR, the NSF NIRT (ECCS-0708765), and the NSF Penn State MRSEC and Center for Nanoscale Science funded this work. We thank Drs. I. Chester of FAR Research, Inc., and R. Awartani of Petra Research, Inc., for providing TMSA. This work was supported in part by World Premier International Research Center (WPI) Initiative on Materials Nanoarchitectonics, MEXT, Japan. Y.S. thanks Iketani Science and Technology Foundation for funding.

Supporting Information Available: Detailed NMR spectra for all new compounds and total energy and atomic coordinates of C_{60} and the molecules listed in Table 1 and Figure 4 inset. This material is available free of charge via the Internet at http://pubs.acs.org.